Supporting Information for

Solution Conformation and Dynamics of the HIV-1 Integrase Core Domain

Nicholas C. Fitzkee[1], James E. Masse[1], Yang Shen[1], David R. Davies[2], and Ad Bax[1]

[1]Laboratory of Chemical Physics
and
[2]Laboratory of Molecular Biology
National Institute of Diabetes and Digestive and Kidney Diseases
National Institutes of Health
5 Memorial Drive
Bethesda, MD 20892

Corresponding author: bax@nih.gov
(301) 496-2848
(301) 402-0907 (Fax)

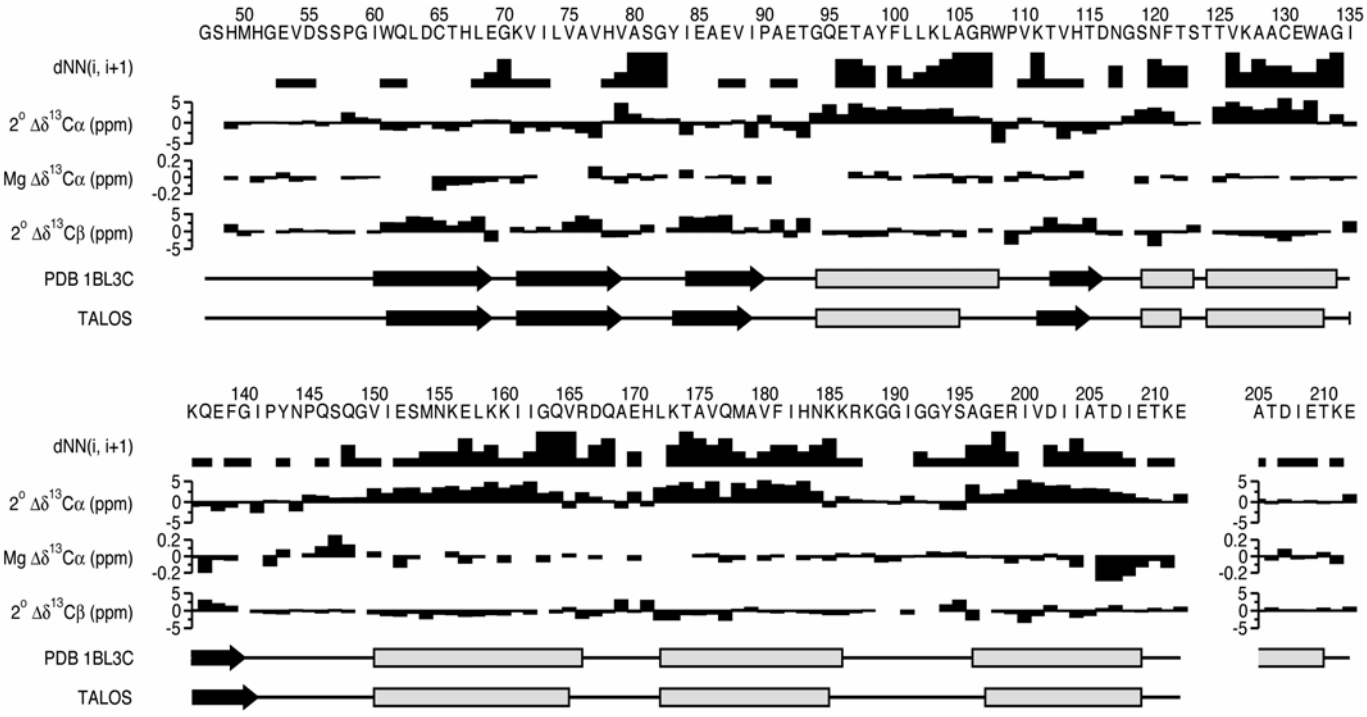

Figure S1. Summary of sequential backbone $^{1}H^{N}$-$^{1}H^{N}$ NOEs (dNN), secondary C^{α} chemical shifts at 40 mM $MgCl_2$ (2^{o} $\Delta\delta$ $^{13}C\alpha$), changes in $^{13}C^{\alpha}$ shifts as $MgCl_2$ concentration is increased from 5 mM to 40 mM (Mg $\Delta\delta$ $^{13}C^{\alpha}$), and secondary C^{β} chemical shifts (2^{o} $\Delta\delta$ $^{13}C^{\beta}$), also at 40 mM $MgCl_2$. The secondary structure from PDB 1BL3 (chain C) is plotted (1), along with the TALOS+ secondary structure predicted from chemical shifts (2). Alternate assignments for residues 205-212 are shown at the bottom right, and chemical shifts indicate that this conformation is disordered. $^{13}C^{\alpha}$ chemical shifts have been adjusted by adding 0.5 ppm to the measured values to account for the ^{2}H isotope effect (3).

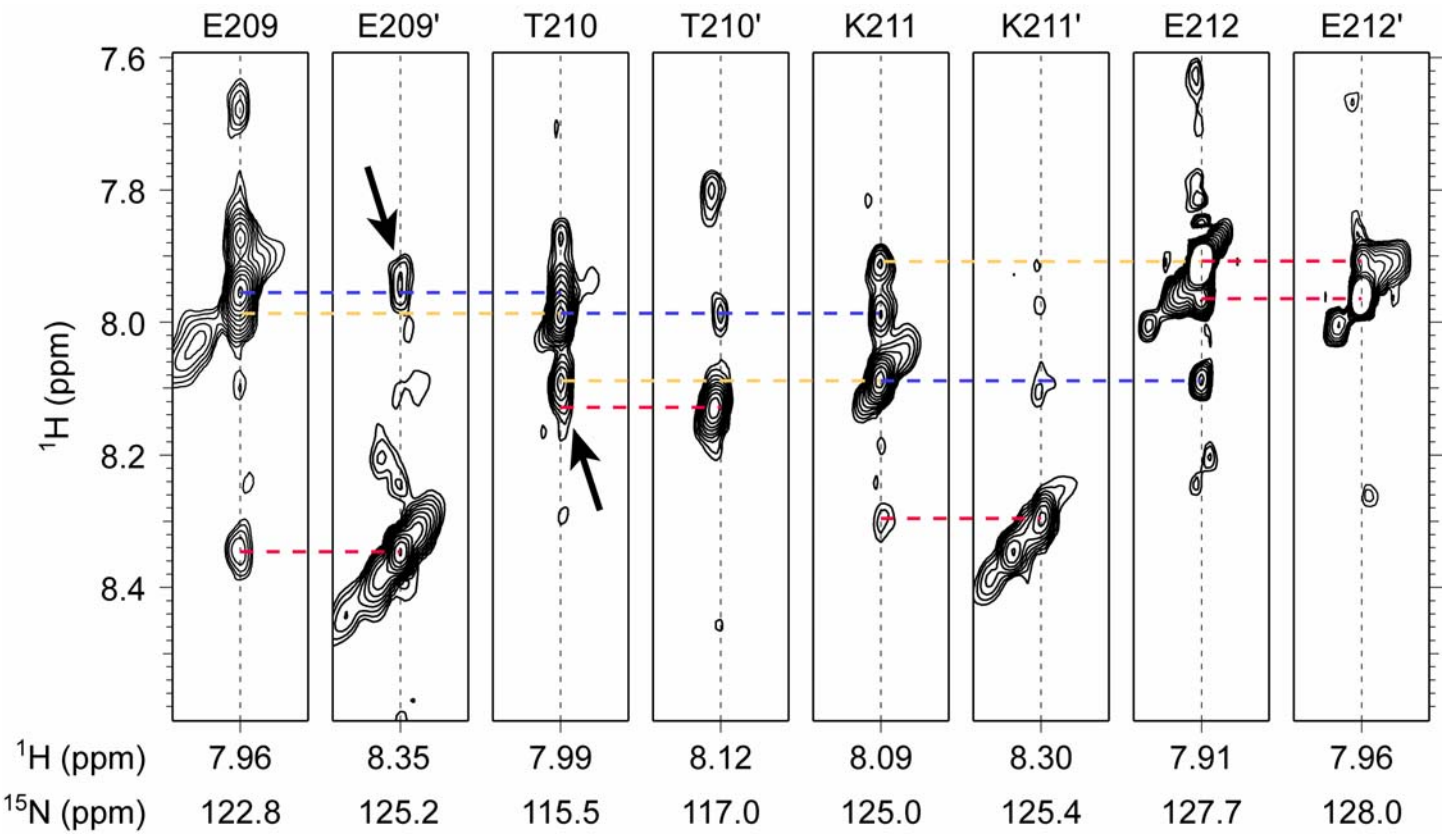

Figure S2. Strip plots taken from a MT-PARE 3D-HMQC NOESY, with ^{1}H and ^{15}N frequencies recorded during t_1 and t_2, respectively, for residues 209-212 of IN$^{50\text{-}212}$ at 800 MHz. Primary and alternate assignment strips are interleaved, and alternate assignments have primed residue indices. Yellow and blue dashed lines indicate connectivity between *i* and *i+1* residues for the primary assignment. The blue lines additionally intersect the alternate assignments at exchange cross peak positions. Red dashed lines indicate the exchange cross peaks between the primary and alternate assignments for these residues. The most unambiguous cross peaks are between residues E209 and E209' (red line), T210 and T210' (blue line), and K211 and K211' (red line). Arrows indicate where cross peaks are obscured by overlap: The highlighted cross peak between E209 and E209' overlaps with a cross peak to I208' (not shown), and the highlighted cross peak between T210 and T210' overlaps with the cross peak between T210 and T211. Additionally, the T210' diagonal peak itself overlaps with the diagonal peak of Q146.

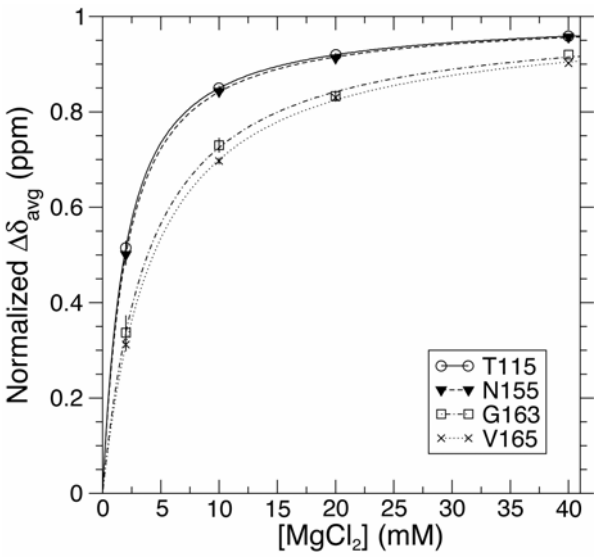

Figure S3. Representative weighted chemical shift changes of $IN^{50\text{-}212}$ as $MgCl_2$ is added to the sample in a series of ^{1}H-^{15}N TROSY-HSQC spectra. The weighted average $\Delta\delta_{avg}$ is calculated as $\sqrt{\frac{1}{2}\left(\Delta\delta_{HN}^2 + \left(\Delta\delta_N / 5\right)^2\right)}$ (4). Residues T115, N155, G163, and V165 are shown. Integrase concentration is fixed at 340 μM, and the fitting methodology as well as approximate K_d values are given in the text. G163 and V165 fit to slightly weaker apparent K_d values, but the uncertainty on these values is much larger than the values for other residues (e.g. G163 has a K_d 3.7 ± 1.0 mM whereas T115 has a K_d of 1.75 ± 0.18 mM). Relatively high uncertainties in fitting results from the fact that neither 0% nor 100% Mg^{2+} ion saturation can be measured directly. Instead, both conditions must be fit in the equation

$$\Delta\delta(L_0) = \Delta\delta(0) + \frac{\left[\left(P_0 + L_0 + K_d\right) - \sqrt{\left(P_0 + L_0 + K_d\right)^2 - 4P_0L_0}\right]}{2P_0}\left(\Delta\delta(\max) - \Delta\delta(0)\right)$$

where P_0 is the total protein concentration, L_0 is the total $MgCl_2$ concentration, $\Delta\delta(0)$ is the chemical shift difference relative to 40 mM $MgCl_2$ when no $MgCl_2$ is present, and $\Delta\delta(\max)$ is the chemical shift change relative to 40 mM $MgCl_2$ when binding is saturated. Many resonances broaden beyond the limit of detection at low MgCl2 concentration, and these resonances typically track with the resonances shown above 10 mM $MgCl_2$. All affected resonances are plotted in figure S5.

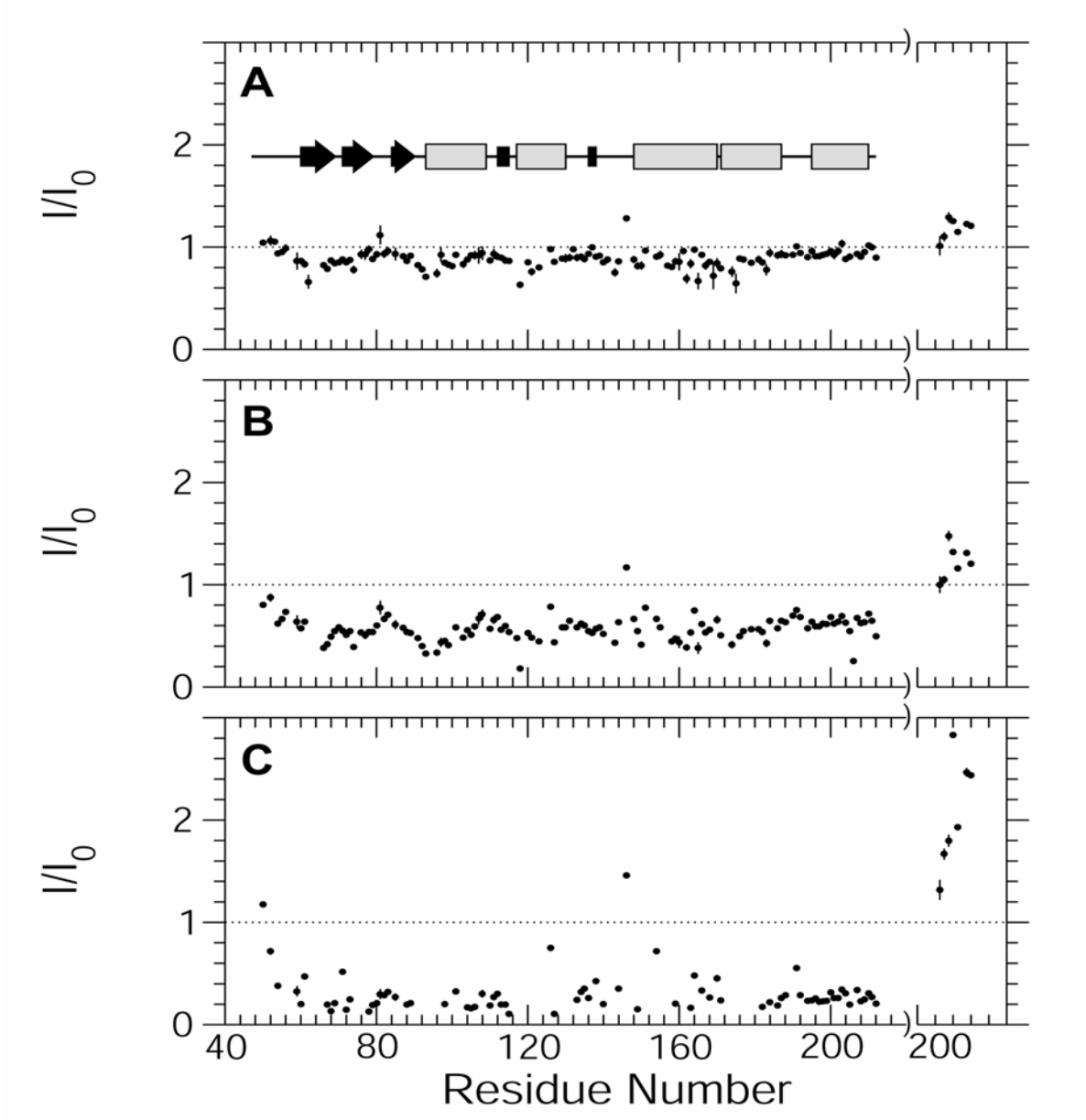

Figure S4. Peak intensities in ^{1}H-^{15}N TROSY-HSQC spectra relative to those of IN^{50-212} in 40 mM $MgCl_2$. Ratios for 20 mM $MgCl_2$ (A), 10 mM MgCl2 (B), and 2 mM $MgCl_2$ (C) are shown, along with the crystallographic secondary structure. Uncertainties are estimated as the spectral noise, and intensity ratios to the right of the axis breaks correspond to effects on alternate assignments for the C-terminus. The intensity of most peaks decrease uniformly as [$MgCl_2$] is lowered, indicating that Mg^{2+} globally stabilizes the core domain. The disordered state of the CT helix is favored under conditions of low $MgCl_2$, as seen from the intensities of alternate assignments for residues 205-212.

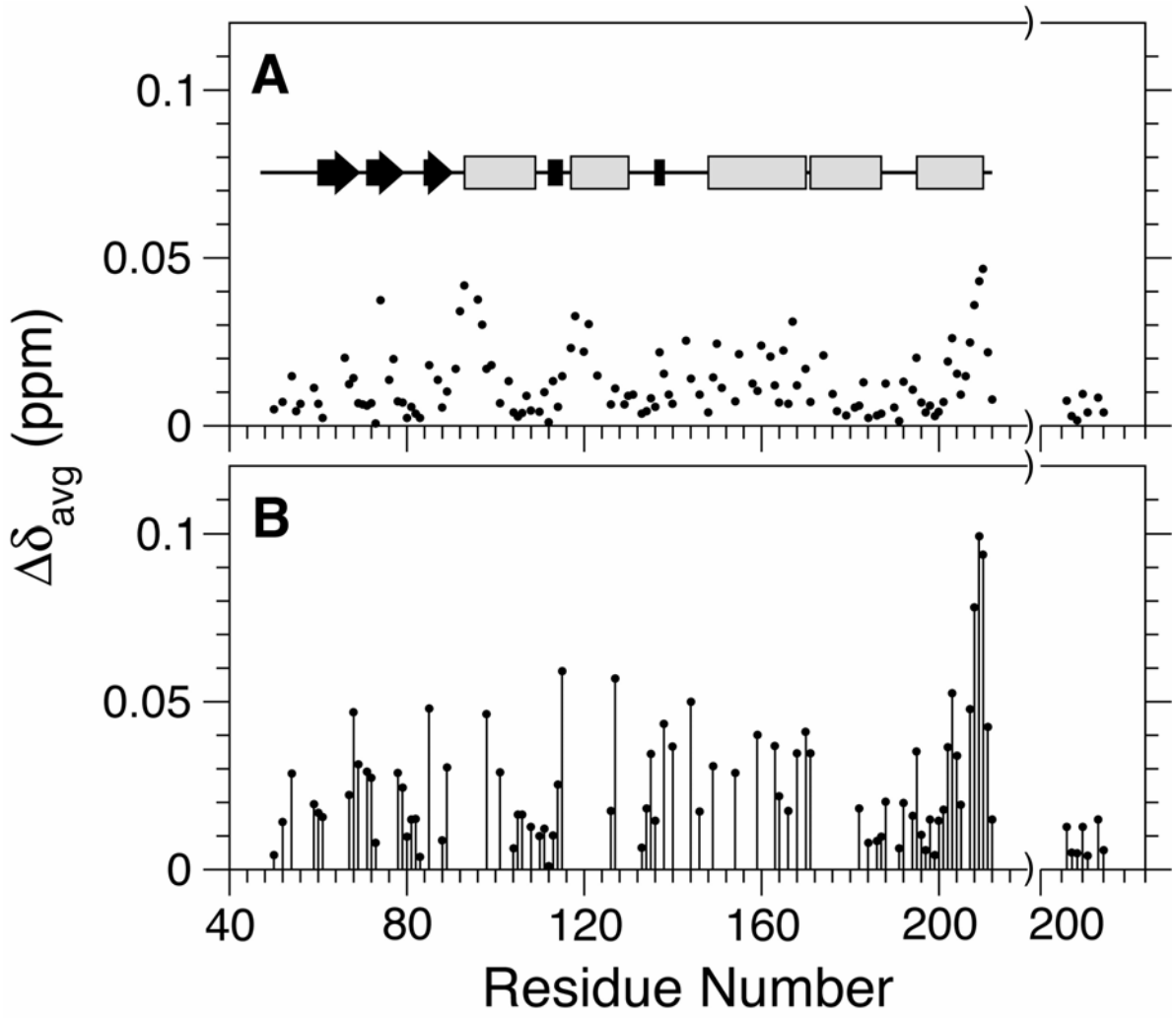

Figure S5. Weighted average chemical shift changes (4) in a ^{1}H-^{15}N TROSY-HSQC spectrum relative to IN^{50-212} in 40 mM $MgCl_2$. Differences for 10 mM $MgCl_2$ (A) and 2 mM $MgCl_2$ (B) are shown, along with the crystallographic secondary structure. Effects on the alternate assignments are plotted to the right of the broken axes. The data suggest that several regions in the catalytic core domain are affected by Mg^{2+} binding, namely residues proximal to the active site (D64, D116, and E152), as well as the CT helix (200-212). The amides of residues D64 and E152 themselves are still broadened at 10 mM $MgCl_2$ and do not become sharp until higher concentrations.

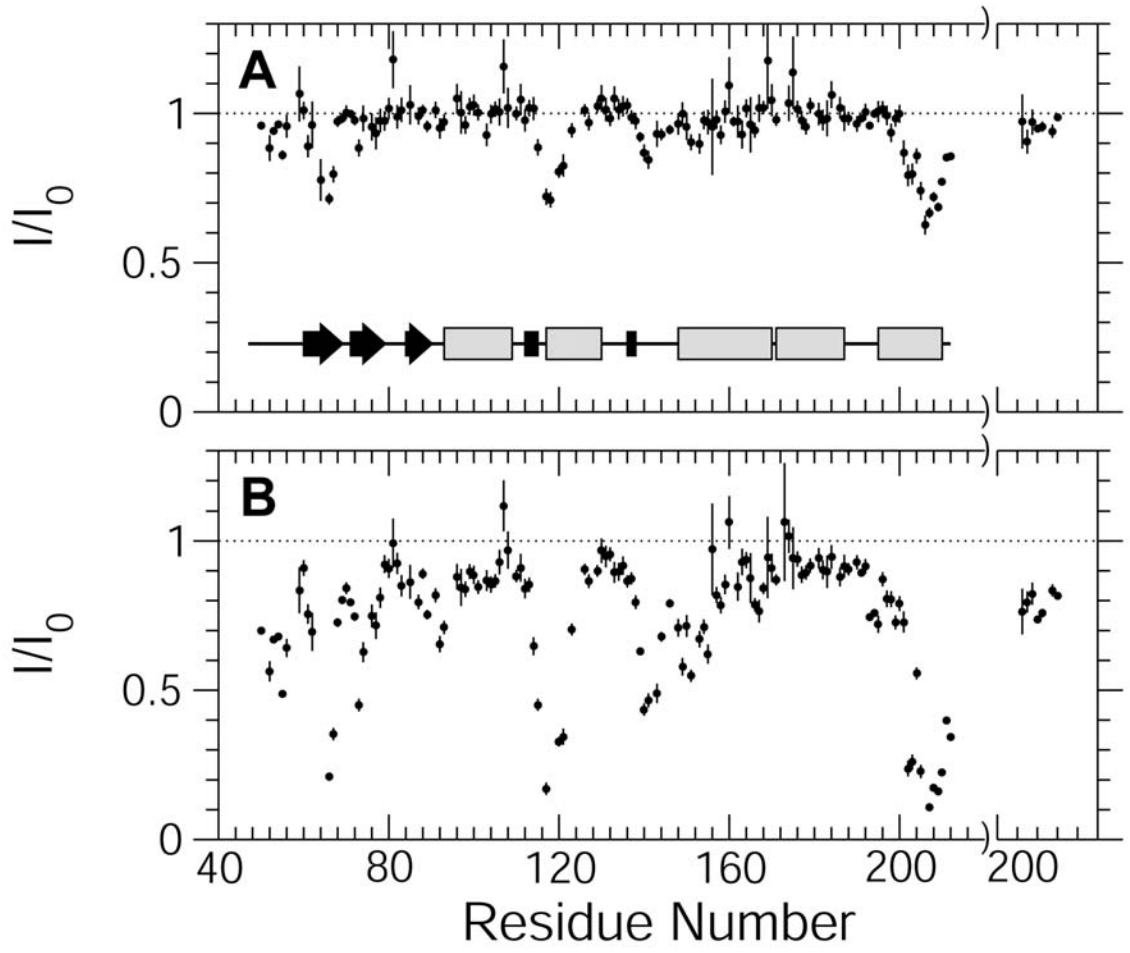

Figure S6. Peak intensity attenuation in a ^{1}H-^{15}N TROSY-HSQC spectrum as $MnCl_2$ is added to $IN^{50\text{-}212}$ in 40 mM $MgCl_2$, resulting from paramagnetic relaxation enhancement of ^{1}H nuclei. Attenuation is measured at 10 μM (A) and 50 μM (B) $MnCl_2$. These profiles indicate binding of Mn^{2+} by the active site residues as well as an additional binding site at the CT helix when this helix is folded, but not when it is disordered. The core domain concentration is 340 μM, indicating that Mn^{2+} is binding in fast exchange both at the active site and at the CT helix.

Figure S7

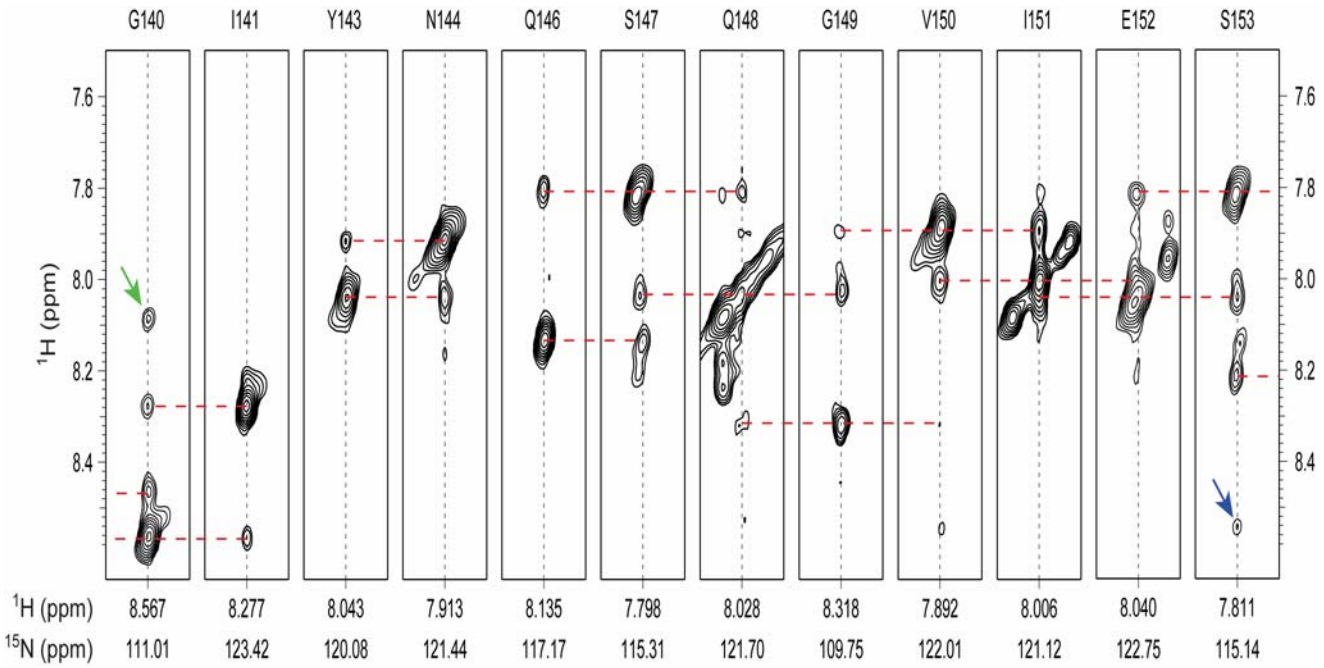

Figure S7. NOESY strips of IN^{50-212} for the catalytic loop residues 140-153. Prolines 142 and 145 interrupt the sequence and are absent from the strip plot. All strips are contoured identically except for Q148 and G149, which are contoured at two-fold lower levels than the other strips. These two resonances are much weaker than the others, because of rapid hydrogen exchange with solvent. Red dashed lines indicate connectivities between diagonal peaks and their associated cross peaks with neighboring residues. In the G140 strip, a green arrow indicates a cross peak with T115 across the beta sheet. In the PDB 1BL3 chain C, the distance between these two protons is 3.04 Å. In the strip for S153, the blue arrow highlights a cross peak with N155. This cross peak arises from spin diffusion through the α4 helix. The other cross peaks, seen in the strips for S147, V150, and S153, arise from overlapped, unrelated resonances. Strip spectra are taken from a MT-PARE 3D-HMQC NOESY, with ^{1}H and ^{15}N frequencies recorded during t_1 and t_2, respectively, with a 150ms mixing time at 800 MHz.

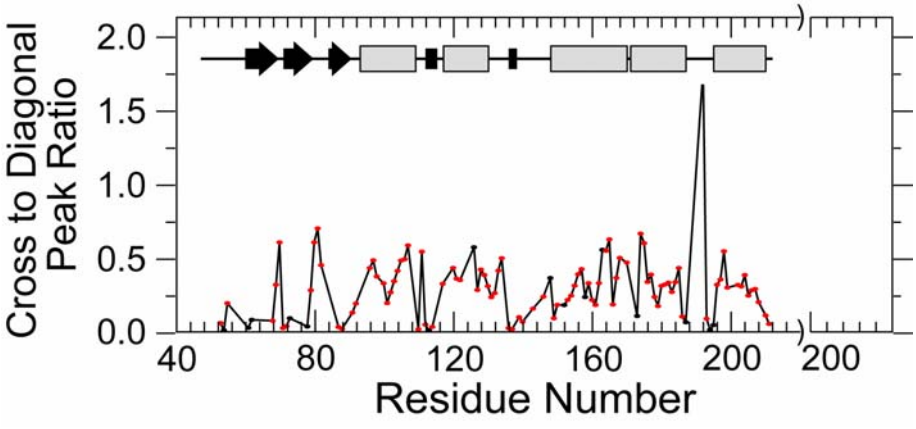

Figure S8. Cross peak to diagonal peak ratios for an H^N-H^N NOESY spectrum in $IN^{50\text{-}212}$. Red points indicate residues where *i* to *i+1* and *i+1* to *i* peaks have been averaged to determine the ratio; black points indicate residues where only one of the peaks could be quantified.

Table S1 – Integrase Core Domain Chemical Shift Assignments[*]

Residue[†]		H_N		N		C'		C_α		C_β	
		δ (ppm)	N[‡]	δ (ppm)	N[‡]	δ (ppm)	N[‡]	δ (ppm)	N[‡]	δ (ppm)	N[‡]
51	H	-	0	-	0	175.501	2	55.644	3	29.206	2
52	G	8.342	7	109.961	7	173.877	4	44.714	6	-	0
53	E	8.296	8	120.571	8	176.527	5	55.907	5	29.006	3
54	V	8.151	8	120.419	8	175.693	5	61.64	5	31.914	3
55	D	8.37	8	124.042	8	175.752	4	53.836	5	40.379	3
56	S	8.158	7	116.512	7	174.068	3	57.201	5	62.921	2
57	S	8.218	7	118.121	7	174.127	2	57.724	2	62.277	1
58	P	-	0	-	0	177.507	2	64.893	2	30.82	2
59	G	8.442	7	105.599	7	174.645	2	45.708	5	-	0
60	I	6.819	5	120.049	5	174.957	3	61.537	5	37.249	3
61	W	8.824	8	127.817	8	175.083	3	55.389	5	31.314	2
62	Q	9.245	6	119.979	6	174.978	3	53.698	3	30.565	3
63	L	8.109	6	121.704	6	175.77	3	53.395	6	45.577	3
64	D	8.948	7	114.971	7	174.219	3	53.352	6	44.141	2
65	C	8.006	6	115.577	6	174.425	4	57.33	5	30.138	3
66	T	9.284	7	120.112	7	171.158	4	59.919	5	69.787	3
67	H	8.014	8	121.458	8	174.709	4	54.858	5	31.913	3
68	L	8.289	7	123.516	7	175.202	4	54.794	5	45.612	3
69	E	9.244	8	121.069	8	175.914	4	56.489	5	26.599	3
70	G	8.725	8	104.823	8	174.192	4	45.087	5	-	0
71	K	8.298	7	121.458	7	174.78	5	53.512	5	32.957	3
72	V	8.474	8	120.769	8	173.714	4	60.975	4	31.24	2
73	I	8.674	7	125.548	6	174.66	2	59.011	4	38.539	2
74	L	8.569	6	130.577	6	-	0	53.566	1	41.635	1
75	V	-	0	-	0	173.431	2	60.562	3	33.82	1
76	A	9.487	5	127.24	5	175.271	2	49.352	3	22.762	2
77	V	9.504	1	118.556	1	174.142	2	58.435	4	34.593	3
78	H	8.836	7	131.413	7	175.374	3	55.777	5	27.882	3
79	V	6.69	5	127.628	5	176.986	3	66.416	5	30.01	3
80	A	8.502	8	117.091	8	177.532	4	53.512	5	17.897	1
81	S	7.151	6	107.844	6	175.339	3	58.612	5	64.336	3
82	G	8.481	7	111.82	7	172.635	3	45.385	5	-	0
83	Y	8.131	6	123.192	6	173.546	3	58.445	5	38.749	2
84	I	7.913	6	122.808	6	174.142	2	58.159	5	41.517	3
85	E	8.737	7	117.347	7	173.982	1	55.566	4	32.918	1

[*] Chemical shifts recorded at 600 MHz field. N and H_N chemical shifts have been corrected by 46 Hz as appropriate to compensate for the TROSY sequences used in assignment. Shifts are not adjusted for the effect of ^2H isotope effects.

[†] Residues with multiple assignments are designated with a "B" appended to the residue number.

[‡] The number of observations across all spectra used in assignment, excluding the HMQC-NOESY spectrum.

Residue†		H_N		N		C'		C_α		C_β	
		δ (ppm)	N‡	δ (ppm)	N‡	δ (ppm)	N‡	δ (ppm)	N‡	δ (ppm)	N‡
86	A	8.311	1	120.427	1	176.078	3	50.599	4	22.615	2
87	E	8.546	8	115.559	8	174.892	3	55.702	5	33.609	3
88	V	8.27	6	123.512	6	176.133	4	62.287	5	31.004	3
89	I	8.692	8	123.256	8	174.451	2	57.466	2	38.392	1
90	P	-	0	-	0	175.825	2	64.25	3	31.055	2
91	A	6.915	6	113.884	6	175.007	4	50.6	5	21.645	3
92	E	9.027	6	124.286	6	175.183	3	54.295	4	27.798	3
93	T	7.618	8	108.805	8	177.88	2	58.242	2	71.877	1
94	G	-	0	-	0	175.458	2	46.774	2	-	0
95	Q	8.922	6	120.879	6	178.995	2	59.528	4	27.537	2
96	E	7.368	7	115.998	7	179.78	3	57.715	5	28.591	2
97	T	7.91	6	117.401	6	174.919	2	66.095	4	67.05	3
98	A	8.897	8	123.835	8	177.828	5	55.001	5	17.284	2
99	Y	7.408	6	116.445	6	176.135	3	60.572	4	36.816	3
100	F	7.429	7	117.28	7	177.482	4	61.154	3	39.234	3
101	L	8.428	7	119.402	7	177.658	3	57.34	5	41.68	2
102	L	8.211	7	118.034	7	179.868	4	57.336	2	40.903	2
103	K	7.425	7	119.1	7	178.847	3	58.963	5	30.958	4
104	L	7.658	7	121.002	7	178.333	4	57.628	5	41.732	3
105	A	8.475	8	116.257	8	178.295	3	52.86	3	17.209	2
106	G	7.652	2	101.548	1	173.993	3	45.945	4	-	0
107	R	7.368	6	121.769	6	174.513	3	56.515	5	30.384	3
108	W	7.54	7	116.77	7	174.791	1	52.289	2	-	0
109	P	-	0	-	0	176.553	3	61.425	3	27.773	2
110	V	9.224	8	131.028	8	174.717	4	62.774	4	30.823	2
111	K	9.033	6	125.624	6	177.169	3	56.036	5	33.147	3
112	T	7.968	7	116.737	7	173.05	3	60.825	5	72.141	3
113	V	8.811	8	120.094	8	173.496	4	58.172	5	33.186	3
114	H	9.091	7	126.788	7	174.879	3	53.849	5	31.038	3
115	T	8.144	7	113.518	7	173.095	3	59.22	5	71.982	2
116	D	8.783	6	117.875	6	174.589	3	52.159	4	39.677	3
117	N	7.857	7	111.827	7	175.992	2	52.316	6	37.122	3
118	G	9.061	7	108.736	7	175.745	1	46.077	2	-	0
119	S	-	0	-	0	175.551	1	60.735	3	62.004	2
120	N	8.663	8	115.168	8	175.959	3	55.971	5	34.12	3
121	F	7.467	7	118.018	7	177.168	3	60.054	5	38.377	3
122	T	7.871	6	108.329	6	174.178	4	61.231	3	68.15	3
123	S	6.755	6	114.836	6	176.456	2	57.66	2	64.3	1
125	T	-	0	-	0	177.039	1	65.286	3	67.866	2
126	V	7.279	8	123.35	8	177.11	3	66.649	5	30.607	3
127	K	7.809	7	123.045	7	178.934	5	59.527	5	31.04	3
128	A	8.282	8	119.427	8	180.772	5	54.489	5	17.488	3

Residue†		H_N		N		C'		C_α		C_β	
		δ (ppm)	N‡	δ (ppm)	N‡	δ (ppm)	N‡	δ (ppm)	N‡	δ (ppm)	N‡
129	A	7.593	7	122.362	7	179.311	4	54.845	5	16.938	2
130	C	8.499	6	115.162	6	177.479	3	64.711	4	24.783	3
131	E	8.645	7	120.066	7	179.569	3	58.882	4	28.149	3
132	W	8.242	7	121.216	7	177.696	3	62.06	3	28.261	3
133	A	8.035	7	115.741	7	176.858	3	51.468	5	18.424	3
134	G	7.778	8	110.022	8	174.329	4	46.459	5	-	0
135	I	8.719	6	121.337	6	175.368	4	60.268	5	40.153	3
136	K	8.539	8	128.459	8	174.709	3	54.884	5	32.09	3
137	Q	8.659	8	124.413	8	175.033	4	54.546	4	31.076	3
138	E	8.47	8	123.901	8	174.431	5	53.951	4	31.038	3
139	F	8.531	8	121.201	8	177.122	5	56.411	5	39.604	3
140	G	8.621	7	110.085	7	173.532	3	44.492	5	-	0
141	I	8.345	7	122.608	7	174.839	2	58.372	2	37.138	1
142	P	-	0	-	0	176.148	2	62.827	3	30.587	2
143	Y	8.106	7	119.21	7	175.108	4	57.719	5	37.208	3
144	N	7.975	7	120.561	7	173.609	2	50.542	2	38.096	1
145	P	-	0	-	0	177.868	3	64.099	3	31.055	2
146	Q	8.204	8	116.374	8	176.768	4	56.56	5	27.796	3
147	S	7.865	7	114.491	7	174.66	2	58.469	5	62.818	3
148	Q	8.091	7	120.88	7	176.717	3	56.101	5	27.882	3
149	G	8.377	7	108.977	7	175.332	4	45.488	5	-	0
150	V	7.957	5	121.203	5	178.312	3	64.85	5	30.605	3
151	I	8.059	7	120.237	7	176.316	3	62.696	5	36.253	2
152	E	8.119	5	121.896	5	179.473	3	59.078	5	27.792	3
153	S	7.884	6	114.332	6	177.248	2	60.936	4	62.096	3
154	M	8.27	7	121.936	7	177.78	3	56.753	5	29.951	3
155	N	8.612	7	119.788	7	177.953	3	55.808	4	37.151	3
156	K	7.533	7	118.511	7	179.486	2	59.394	4	31.04	3
157	E	7.941	7	121.075	7	178.547	3	58.508	5	27.734	3
158	L	8.789	7	119.531	7	178.718	2	57.719	5	40.218	3
159	K	7.922	7	115.619	7	179.064	3	60.372	5	31.019	2
160	K	7.763	6	121.053	6	179.456	4	58.948	5	30.924	1
161	I	8.183	7	120.43	7	178.93	2	64.643	5	37.359	2
162	I	8.75	5	119.457	5	177.766	2	65.497	5	36.718	2
163	G	7.744	6	102.965	4	175.983	4	46.498	5	-	0
164	Q	7.717	6	119.401	6	178.246	3	57.576	5	27.765	2
165	V	7.66	6	109.983	6	177.349	3	60.507	5	32.012	3
166	R	7.765	8	122.294	8	177.121	4	57.719	5	27.766	3
167	D	8.383	8	113.746	8	177.113	4	54.509	5	38.987	3
168	Q	8.179	8	117.666	8	174.749	4	55.493	5	27.846	3
169	A	7.519	7	120.815	7	176.258	3	50.238	5	21.435	2
170	E	8.409	6	120.036	6	177.19	3	58.146	5	28.899	3

Residue†		H_N		N		C'		C_α		C_β	
		δ (ppm)	N‡	δ (ppm)	N‡	δ (ppm)	N‡	δ (ppm)	N‡	δ (ppm)	N‡
171	H	7.869	8	115.836	8	176.133	2	54.748	2	32.051	1
172	L	-	0	-	0	178.607	2	57.607	3	39.117	1
173	K	9.429	6	115.612	6	178.38	3	59.55	5	29.516	3
174	T	7.059	5	117.668	7	175.538	3	66.151	4	67.385	3
175	A	7.525	7	124.532	7	178.895	4	54.548	5	17.444	3
176	V	8.566	7	115.221	7	176.695	5	66.519	5	30.533	3
177	Q	7.061	7	114.008	8	180.196	3	56.23	2	25.637	2
178	M	8.253	3	120.312	3	176.911	4	59.141	4	32.28	3
179	A	8.146	7	120.808	7	178.856	3	54.535	5	19.236	3
180	V	8.313	8	119.336	8	176.725	3	66.843	5	31.067	3
181	F	7.895	7	119.064	7	176.597	3	61.588	5	38.042	3
182	I	8.698	7	118.43	7	179.219	3	64.643	5	37.404	3
183	H	8.823	7	116.833	7	177.668	3	60.359	5	28.874	3
184	N	8.948	7	116.513	7	177.159	2	54.93	3	37.377	3
185	K	7.893	7	114.522	6	177.761	3	54.748	4	31.059	3
186	K	7.159	8	120.619	8	176.537	4	56.877	5	31.055	2
187	R	8.732	7	126.92	7	176.174	5	55.977	5	29.403	3
188	K	8.033	8	124.545	8	176.765	3	55.966	4	32.051	1
189	G	8.52	4	110.342	4	174.515	2	44.671	4	-	0
190	G	8.107	8	108.484	8	174.521	4	44.236	6	-	0
191	I	8.245	7	121.384	7	177.485	5	62.06	5	36.669	3
192	G	8.653	8	113.141	8	174.651	5	44.735	4	-	0
193	G	7.888	5	108.11	5	173.221	3	44.473	4	-	0
194	Y	7.731	8	117.281	8	176.456	5	55.977	4	39.468	3
195	S	8.813	8	117.797	8	175.298	5	56.054	4	65.521	3
196	A	9.85	7	125.634	7	179.73	5	55.493	5	16.054	2
197	G	8.969	7	102.323	5	175.882	4	46.226	5	-	0
198	E	7.504	6	119.923	6	178.265	4	57.68	5	28.924	3
199	R	8.647	8	119.468	8	178.397	3	58.405	5	29.121	3
200	I	8.307	7	117.216	7	175.565	2	65.93	3	34.295	2
201	V	6.149	1	119.134	1	176.602	3	66.243	4	30.107	2
202	D	7.831	6	118.586	6	179.051	3	57.194	4	41.58	3
203	I	8.522	7	119.608	7	178.935	3	64.635	5	37.441	3
204	I	8.35	7	119.945	7	178.165	3	63.814	5	35.772	3
204B	I	-	0	-	0	175.889	2	60.428	2	37.385	2
205	A	8.819	8	122.296	8	180.152	4	54.613	5	17.299	2
205B	A	8.316	7	128.002	7	177.61	4	52.03	5	18.415	3
206	T	7.888	7	112.181	7	175.292	3	64.526	5	68.776	3
206B	T	8.06	8	112.852	8	174.227	3	61.342	5	68.947	3
207	D	7.728	8	122.601	8	177.052	5	55.648	5	41.586	3
207B	D	8.316	6	122.294	6	176.01	3	53.886	5	40.392	3
208	I	7.935	8	118.454	8	177.088	2	62.572	5	37.406	3

Residue†		H_N δ (ppm)	N‡	N δ (ppm)	N‡	C' δ (ppm)	N‡	C_α δ (ppm)	N‡	C_β δ (ppm)	N‡
208B	I	7.981	8	120.109	8	176.198	4	60.777	5	37.582	3
209	E	8.014	8	121.908	8	176.982	4	56.683	5	29.019	3
209B	E	8.409	8	124.284	8	176.488	4	56.042	3	29.229	4
210	T	8.047	8	114.586	8	174.521	5	61.977	5	68.835	3
210B	T	8.185	7	116.24	7	174.224	5	61.407	5	68.923	3
211	K	8.146	8	124.157	8	175.621	5	55.777	5	32.014	3
211B	K	8.356	7	124.479	7	175.538	5	55.704	5	32.014	3
212	E	7.971	8	126.848	8	181.115	2	57.595	2	30.031	1
212B	E	8.021	8	127.174	8	181.05	2	57.53	2	30.031	1

Table S2 – ^{15}N Relaxation Data

600 MHz Relaxation Data (R_1, R_2, NOE)

Residue[†]		R_1 (s^{-1})	σ_{R1} (s^{-1}) [‡]	R_2 (s^{-1})	σ_{R2} (s^{-1})[‡]	NOE	σ_{NOE}[‡]
51	H	-	-	-	-	-	-
52	G	1.38	0.09	5.6	0.9	-0.15	0.09
53	E	1.48	0.02	6.1	0.1	-	-
54	V	1.40	0.01	7.6	0.1	-	-
55	D	1.42	0.03	8.9	0.3	0.33	0.03
56	S	1.27	0.06	11.1	0.8	0.39	0.07
57	S	1.21	0.04	14.2	0.6	-	-
58	P	-	-	-	-	-	-
59	G	0.69	0.11	24.0	4.3	0.62	0.12
60	I	0.78	0.05	27.6	2.1	0.73	0.07
61	W	0.64	0.09	32.5	7.7	0.92	0.07
62	Q	0.57	0.20	23.6	11.0	0.67	0.08
63	L	-	-	-	-	-	-
64	D	0.95	0.36	28.7	21.0	0.91	0.10
65	C	0.65	0.24	30.0	10.3	0.69	0.11
66	T	0.65	0.03	28.3	1.6	0.76	0.04
67	H	-	-	-	-	0.71	0.07
68	L	0.66	0.03	26.5	1.3	0.81	0.04
69	E	0.75	0.03	25.3	1.2	0.70	0.04
70	G	0.82	0.04	26.8	1.5	0.71	0.05
71	K	0.67	0.03	26.4	1.1	0.65	0.03
72	V	0.62	0.03	27.4	1.2	0.69	0.03
73	I	-	-	-	-	0.70	0.08
74	L	-	-	-	-	0.82	0.08
75	V	-	-	-	-	-	-
76	A	-	-	-	-	0.86	0.08
77	V	-	-	-	-	0.69	0.09
78	H	0.50	0.22	25.7	14.5	0.91	0.06
79	V	0.72	0.06	28.8	2.7	0.63	0.05
80	A	0.65	0.07	24.2	2.9	0.60	0.07
81	S	0.62	0.16	23.9	6.2	0.98	0.15
82	G	0.63	0.09	26.1	3.8	0.87	0.08
83	Y	0.75	0.09	29.8	4.2	0.78	0.08
84	I	-	-	-	-	-	-
85	E	0.79	0.44	29.5	20.3	0.78	0.09

[†] Residues with multiple assignments are designated with a "B" appended to the residue number. Relaxation data are recorded at 298K, pH 6.8 in 40 mM $MgCl_2$. Exact buffers are described in the text.
[‡] Uncertainties are given as the 66% confidence interval obtained using standard error propagation formulae.

Residue†		R_1 (s^{-1})	σ_{R1} (s^{-1}) ‡	R_2 (s^{-1})	σ_{R2} (s^{-1})‡	NOE	σ_{NOE}‡
86	A	-	-	-	-	-	-
87	E	0.77	0.14	24.6	6.6	0.72	0.04
88	V	0.75	0.04	26.4	1.4	0.70	0.04
89	I	0.67	0.04	28.1	1.9	0.77	0.03
90	P	-	-	-	-	-	-
91	A	0.63	0.04	28.3	1.6	0.63	0.04
92	E	0.73	0.05	26.3	2.2	0.77	0.07
93	T	0.72	0.04	28.6	1.9	0.78	0.05
94	G	-	-	-	-	-	-
95	Q	-	-	-	-	-	-
96	E	0.66	0.08	29.0	3.8	0.68	0.08
97	T	0.56	0.14	27.2	6.4	0.90	0.13
98	A	0.78	0.06	28.0	3.0	0.90	0.07
99	Y	0.61	0.05	28.9	2.3	0.80	0.06
100	F	0.67	0.08	28.2	3.9	1.05	0.08
101	L	0.69	0.27	21.4	9.9	0.79	0.04
102	L	-	-	-	-	-	-
103	K	0.87	0.21	28.1	9.8	0.83	0.07
104	L	0.58	0.18	41.2	15.9	0.78	0.06
105	A	0.67	0.06	28.2	3.1	0.80	0.05
106	G	0.70	0.07	28.1	3.0	0.74	0.07
107	R	0.69	0.11	32.7	5.2	0.97	0.18
108	W	0.51	0.11	22.8	5.3	0.69	0.10
109	P	-	-	-	-	-	-
110	V	0.76	0.04	24.6	1.4	0.60	0.04
111	K	0.75	0.10	25.0	4.2	0.74	0.07
112	T	0.67	0.06	26.2	2.6	0.81	0.07
113	V	0.69	0.04	27.7	2.0	0.80	0.04
114	H	0.67	0.06	27.9	3.0	0.73	0.05
115	T	0.69	0.05	27.1	2.1	0.81	0.07
116	D	0.60	0.12	30.7	6.6	-	-
117	N	0.64	0.05	26.0	2.1	0.89	0.08
118	G	0.72	0.05	28.2	2.0	0.78	0.06
119	S	-	-	-	-	-	-
120	N	0.73	0.04	27.8	1.6	0.78	0.05
121	F	0.60	0.06	30.1	3.2	0.69	0.08
122	T	0.70	0.06	26.3	2.5	-	-
123	S	0.65	0.04	22.2	1.4	0.61	0.05
125	T	-	-	-	-	-	-
126	V	0.70	0.04	26.0	1.8	0.74	0.05
127	K	0.69	0.04	26.4	1.7	0.73	0.05
128	A	-	-	-	-	-	-

Residue†		R_1 (s^{-1})	σ_{R1} (s^{-1}) ‡	R_2 (s^{-1})	σ_{R2} (s^{-1})‡	NOE	σ_{NOE}‡
129	A	0.68	0.04	28.1	1.7	0.76	0.04
130	C	0.66	0.08	27.9	3.5	0.78	0.06
131	E	0.62	0.08	28.1	3.5	0.80	0.06
132	W	0.66	0.08	24.7	3.1	-	-
133	A	0.60	0.08	24.8	3.0	0.89	0.07
134	G	0.64	0.05	27.9	2.3	0.88	0.05
135	I	0.62	0.06	23.2	2.4	0.91	0.05
136	K	0.69	0.05	27.9	2.1	0.77	0.03
137	Q	0.63	0.04	27.3	1.7	0.83	0.04
138	E	0.65	0.04	27.1	1.9	0.74	0.05
139	F	0.65	0.03	25.6	1.1	0.79	0.04
140	G	0.89	0.04	19.5	1.0	0.43	0.05
141	I	0.99	0.06	23.9	1.8	0.42	0.06
142	P	-	-	-	-	-	-
143	Y	0.98	0.06	21.0	1.6	0.53	0.07
144	N	1.05	0.04	19.7	0.9	0.52	0.05
145	P	-	-	-	-	-	-
146	Q	1.10	0.04	18.0	0.7	-	-
147	S	1.06	0.07	18.2	1.4	-	-
148	Q	1.16	0.07	16.9	1.4	0.59	0.07
149	G	1.00	0.07	19.0	1.5	0.54	0.07
150	V	0.95	0.08	22.2	2.3	-	-
151	I	0.71	0.06	25.5	2.5	0.68	0.06
152	E	0.76	0.12	30.9	5.7	-	-
153	S	0.79	0.07	25.6	2.5	-	-
154	M	0.78	0.08	26.5	2.9	0.69	0.06
155	N	0.74	0.08	29.2	3.8	0.94	0.10
156	K	0.66	0.16	26.9	7.3	0.77	0.13
157	E	0.61	0.07	27.9	3.2	-	-
158	L	0.64	0.08	28.4	3.6	0.77	0.06
159	K	0.66	0.08	28.8	3.3	0.83	0.06
160	K	0.64	0.11	25.8	4.4	0.77	0.08
161	I	0.68	0.09	29.5	4.0	-	-
162	I	0.69	0.12	31.4	6.0	0.81	0.06
163	G	0.67	0.09	24.4	3.8	0.75	0.05
164	Q	0.64	0.05	27.6	2.3	0.75	0.04
165	V	0.63	0.21	39.4	16.4	0.73	0.10
166	R	0.70	0.06	24.0	2.3	0.74	0.04
167	D	0.63	0.08	32.3	4.6	0.74	0.08
168	Q	0.69	0.04	27.2	1.8	0.80	0.05
169	A	0.59	0.12	29.0	5.8	0.58	0.12
170	E	0.91	0.11	22.8	3.7	0.44	0.06

Residue†		R_1 (s^{-1})	σ_{R1} (s^{-1}) ‡	R_2 (s^{-1})	σ_{R2} (s^{-1})‡	NOE	σ_{NOE}‡
171	H	0.82	0.03	22.5	1.0	0.35	0.04
172	L	-	-	-	-	-	-
173	K	0.65	0.16	28.2	7.7	0.77	0.14
174	T	0.63	0.09	32.9	5.3	0.81	0.10
175	A	0.57	0.11	28.0	5.6	-	-
176	V	0.77	0.07	28.7	2.5	0.86	0.05
177	Q	0.68	0.07	29.9	3.6	0.86	0.06
178	M	0.49	0.09	26.4	4.3	-	-
179	A	0.74	0.05	20.8	1.4	-	-
180	V	0.58	0.08	26.6	3.4	0.54	0.04
181	F	0.67	0.07	27.9	3.0	0.82	0.07
182	I	0.66	0.07	26.9	3.1	0.89	0.06
183	H	0.79	0.11	36.5	6.9	0.69	0.08
184	N	0.62	0.07	29.6	3.9	0.83	0.07
185	K	0.78	0.07	29.8	3.2	-	-
186	K	0.68	0.06	31.1	2.9	0.88	0.08
187	R	0.83	0.06	25.6	2.2	0.69	0.07
188	K	1.03	0.04	19.4	0.8	0.54	0.05
189	G	-	-	-	-	-	-
190	G	1.20	0.03	11.3	0.4	0.35	0.05
191	I	1.13	0.02	12.8	0.4	-	-
192	G	1.20	0.04	12.3	0.6	0.30	0.05
193	G	1.22	0.02	14.2	0.3	-	-
194	Y	1.00	0.02	18.4	0.5	0.37	0.03
195	S	0.78	0.04	25.4	1.6	-	-
196	A	0.70	0.05	27.7	2.5	0.76	0.06
197	G	0.74	0.07	28.5	3.1	0.85	0.07
198	E	0.75	0.06	21.8	2.2	0.69	0.06
199	R	0.78	0.07	25.9	2.6	0.70	0.05
200	I	0.76	0.07	26.9	2.6	0.82	0.06
201	V	0.75	0.07	21.2	2.6	0.86	0.09
202	D	0.87	0.09	29.6	3.6	0.82	0.08
203	I	0.76	0.08	26.7	3.5	0.76	0.07
204	I	-	-	-	-	-	-
204B	I	-	-	-	-	-	-
205	A	0.72	0.07	28.1	3.0	0.66	0.06
205B	A	2.12	1.59	7.5	10.7	-	-
206	T	0.69	0.06	27.1	2.5	0.79	0.08
206B	T	1.43	0.45	5.1	3.6	-0.21	-0.10
207	D	0.88	0.04	22.5	1.2	0.59	0.04
207B	D	1.48	0.32	8.1	3.1	0.19	0.09
208	I	0.98	0.03	19.3	0.7	0.44	0.04

Residue†		R_1 (s^{-1})	σ_{R1} (s^{-1}) ‡	R_2 (s^{-1})	σ_{R2} (s^{-1})‡	NOE	σ_{NOE}‡
208B	I	1.44	0.08	5.4	0.7	0.13	0.03
209	E	1.11	0.03	18.5	0.7	0.52	0.05
209B	E	1.60	0.18	4.6	1.5	-0.12	0.04
210	T	1.27	0.02	12.3	0.3	0.31	0.03
210B	T	1.36	0.16	2.0	1.2	-	-
211	K	1.42	0.02	7.7	0.2	0.11	0.02
211B	K	1.25	0.10	2.7	0.9	-0.52	0.06
212	E	1.29	0.01	2.9	0.1	-0.17	0.01
212B	E	1.15	0.03	2.0	0.3	-0.63	0.03

900 MHz Relaxation Data (R_1, R_2)

Residue[†]		R_1 (s^{-1})	σ_{R1} (s^{-1})[‡]	R_2 (s^{-1})	σ_{R2} (s^{-1})[‡]
51	H	-	-	-	-
52	G	1.20	0.13	8.5	0.8
53	E	1.30	0.02	7.9	0.1
54	V	1.20	0.02	10.3	0.1
55	D	1.17	0.04	13.7	0.2
56	S	0.92	0.08	16.0	0.8
57	S	0.93	0.05	18.6	0.6
58	P	-	-	-	-
59	G	0.64	0.17	37.9	7.5
60	I	0.47	0.04	37.1	2.0
61	W	0.43	0.10	33.7	7.0
62	Q	0.42	0.46	26.2	20.1
63	L	-	-	-	-
64	D	-	-	-	-
65	C	-	-	-	-
66	T	0.42	0.04	38.8	2.4
67	H	-	-	-	-
68	L	-	-	-	-
69	E	0.49	0.04	35.5	1.5
70	G	0.52	0.05	33.5	2.2
71	K	0.44	0.03	37.5	1.3
72	V	0.40	0.03	36.3	1.3
73	I	-	-	-	-
74	L	-	-	-	-
75	V	-	-	-	-
76	A	-	-	-	-
77	V	-	-	-	-
78	H	0.57	0.32	34.2	21.9
79	V	0.41	0.05	37.9	3.1
80	A	0.43	0.08	35.1	3.8
81	S	0.60	0.20	31.9	6.8
82	G	0.42	0.09	35.4	4.5
83	Y	0.40	0.13	44.9	9.5
84	I	-	-	-	-
85	E	-	-	-	-
86	A	-	-	-	-
87	E	0.44	0.13	42.0	9.0

[†] Residues with multiple assignments are designated with a "B" appended to the residue number. Relaxation data are recorded at 298K, pH 6.8 in 40 mM $MgCl_2$. Exact buffers are described in the text.
[‡] Uncertainties are given as the 66% confidence interval obtained using standard error propagation formulae.

Residue†		R_1 (s^{-1})	σ_{R1} (s^{-1})‡	R_2 (s^{-1})	σ_{R2} (s^{-1})‡
88	V	0.27	0.39	35.5	1.9
89	I	0.43	0.04	41.3	2.4
90	P	-	-	-	-
91	A	0.46	0.04	38.0	2.0
92	E	0.50	0.07	38.7	4.1
93	T	0.47	0.07	35.8	2.9
94	G	-	-	-	-
95	Q	-	-	-	-
96	E	0.62	0.14	34.1	5.9
97	T	0.63	0.22	32.6	7.9
98	A	0.42	0.07	37.9	3.6
99	Y	0.42	0.05	35.5	2.5
100	F	0.48	0.09	40.7	5.3
101	L	0.46	0.33	46.6	26.3
102	L	-	-	-	-
103	K	0.35	0.21	40.5	15.7
104	L	0.29	0.19	27.6	8.0
105	A	0.49	0.06	39.7	3.8
106	G	0.45	0.09	34.9	4.1
107	R	0.31	0.13	49.8	10.7
108	W	0.76	0.22	28.8	6.7
109	P	-	-	-	-
110	V	0.45	0.05	26.5	2.1
111	K	0.55	0.14	35.2	5.9
112	T	0.36	0.06	34.8	2.8
113	V	0.40	0.05	39.7	2.7
114	H	0.35	0.08	44.6	5.4
115	T	0.38	0.06	43.4	4.2
116	D	0.58	0.37	45.5	20.2
117	N	0.42	0.07	37.1	3.6
118	G	0.61	0.11	37.3	4.2
119	S	-	-	-	-
120	N	0.48	0.05	40.0	2.6
121	F	0.53	0.08	35.1	4.0
122	T	0.35	0.07	37.4	3.7
123	S	0.48	0.04	33.0	1.5
125	T	-	-	-	-
126	V	0.41	0.04	35.6	2.0
127	K	0.43	0.05	37.6	2.5
128	A	-	-	-	-
129	A	0.40	0.04	37.7	2.0
130	C	0.33	0.08	34.8	3.8

Residue†		R_1 (s^{-1})	σ_{R1} (s^{-1})‡	R_2 (s^{-1})	σ_{R2} (s^{-1})‡
131	E	0.28	0.07	34.9	3.7
132	W	0.33	0.09	34.2	4.5
133	A	0.46	0.10	37.5	4.2
134	G	0.46	0.06	37.3	2.9
135	I	0.36	0.06	35.4	3.0
136	K	0.37	0.05	37.2	2.9
137	Q	0.42	0.04	38.9	2.3
138	E	0.41	0.05	36.8	2.4
139	F	0.43	0.03	34.8	1.2
140	G	0.58	0.06	26.1	1.6
141	I	0.72	0.15	37.7	4.9
142	P	-	-	-	-
143	Y	0.77	0.16	30.8	4.0
144	N	0.80	0.06	28.8	1.4
145	P	-	-	-	-
146	Q	0.80	0.04	23.1	0.8
147	S	0.83	0.10	26.3	1.9
148	Q	0.87	0.10	23.4	1.8
149	G	0.76	0.11	28.6	2.7
150	V	0.61	0.14	36.2	5.7
151	I	0.50	0.09	35.2	4.1
152	E	0.51	0.30	53.9	25.8
153	S	0.60	0.08	32.4	3.1
154	M	0.51	0.11	39.3	5.4
155	N	0.41	0.10	40.5	5.7
156	K	0.18	0.38	43.5	26.9
157	E	0.40	0.10	38.7	5.5
158	L	0.52	0.11	38.1	5.2
159	K	0.47	0.10	36.3	4.8
160	K	0.38	0.22	46.9	15.9
161	I	0.37	0.13	35.9	6.9
162	I	0.59	0.21	41.0	11.6
163	G	0.47	0.17	44.4	12.6
164	Q	0.46	0.06	36.5	3.0
165	V	-	-	-	-
166	R	0.48	0.07	40.5	4.1
167	D	0.62	0.22	56.8	19.1
168	Q	0.45	0.05	36.1	2.5
169	A	-	-	-	-
170	E	0.44	0.18	40.3	11.5
171	H	0.60	0.05	33.0	1.5
172	L	-	-	-	-

Residue†		R_1 (s^{-1})	σ_{R1} (s^{-1})‡	R_2 (s^{-1})	σ_{R2} (s^{-1})‡
173	K	-	-	-	-
174	T	0.48	0.13	40.9	7.8
175	A	0.42	0.22	33.1	9.6
176	V	0.41	0.06	35.5	2.5
177	Q	0.50	0.07	37.5	3.4
178	M	0.51	0.09	43.3	5.8
179	A	0.51	0.27	28.5	1.8
180	V	0.36	0.07	40.3	5.3
181	F	0.35	0.07	36.2	3.7
182	I	0.40	0.07	38.2	4.0
183	H	0.38	0.15	43.0	12.0
184	N	0.45	0.10	37.9	5.3
185	K	0.44	0.08	37.6	4.2
186	K	0.50	0.07	37.0	3.6
187	R	0.53	0.09	37.7	4.0
188	K	0.71	0.04	25.3	0.8
189	G	-	-	-	-
190	G	1.04	0.04	13.2	0.4
191	I	0.89	0.03	17.9	0.3
192	G	0.91	0.04	16.7	0.5
193	G	0.95	0.02	19.7	0.3
194	Y	0.78	0.03	25.3	0.5
195	S	0.52	0.05	36.1	2.1
196	A	0.42	0.07	35.5	3.4
197	G	0.32	0.10	29.9	4.5
198	E	0.53	0.06	31.0	2.4
199	R	0.52	0.06	34.6	2.7
200	I	0.44	0.06	36.8	3.2
201	V	0.51	0.08	39.1	4.2
202	D	0.41	0.09	39.8	4.8
203	I	0.30	0.08	38.6	4.6
204	I	-	-	-	-
204B	I	-	-	-	-
205	A	0.54	0.09	37.8	4.4
205B	A	-	-	-	-
206	T	0.46	0.09	35.9	3.5
206B	T	1.52	0.95	8.6	3.0
207	D	0.60	0.05	30.2	1.4
207B	D	1.26	0.45	8.8	2.3
208	I	0.74	0.04	27.2	0.9
208B	I	1.22	0.13	7.5	0.6
209	E	0.94	0.06	26.2	0.9

Residue[†]		R_1 (s^{-1})	σ_{R1} (s^{-1})[‡]	R_2 (s^{-1})	σ_{R2} (s^{-1})[‡]
209B	E	1.64	0.39	6.1	1.1
210	T	1.08	0.03	17.6	0.3
210B	T	1.49	0.30	3.7	0.9
211	K	1.20	0.03	11.6	0.2
211B	K	1.29	0.18	3.7	0.7
212	E	1.23	0.01	5.2	0.1
212B	E	1.17	0.05	2.0	0.2

References

1. Maignan, S., Guilloteau, J. P., Zhou-Liu, Q., Clement-Mella, C., and Mikol, V. (1998) *J Mol Biol* **282**, 359-368
2. Shen, Y., Delaglio, F., Cornilescu, G., and Bax, A. (2009) *J Biomol NMR* **44**, 213-223
3. Garrett, D. S., Seok, Y. J., Liao, D. I., Peterkofsky, A., Gronenborn, A. M., and Clore, G. M. (1997) *Biochemistry* **36**, 2517-2530
4. Grzesiek, S., Bax, A., Hu, J. S., Kaufman, J., Palmer, I., Stahl, S. J., Tjandra, N., and Wingfield, P. T. (1997) *Protein Sci* **6**, 1248-1263